THE JOURNAL OF BIOLOGICAL CHEMISTRY VOL. 283, NO. 32, pp. 22113–22120, August 8, 2008

Structure-Function Analysis of the C3 Binding Region of *Staphylococcus aureus* Immune Subversion Protein Sbi*[S]

Received for publication, April 4, 2008, and in revised form, May 19, 2008 Published, JBC Papers in Press, June 11, 2008, DOI 10.1074/jbc.M802636200

Abhishek Upadhyay[‡], Julia D. Burman[‡], Elizabeth A. Clark[‡1], Elisa Leung[§], David E. Isenman[§], Jean M. H. van den Elsen[‡2], and Stefan Bagby[‡3]

From the [‡]Department of Biology and Biochemistry, University of Bath, Bath BA2 7AY, United Kingdom and the [§]Department of Biochemistry, University of Toronto, Toronto, Ontario M5S 1A8, Canada

Among the recently discovered *Staphylococcus aureus* immune evasion proteins, Sbi is unique in its ability to interact with components of both the adaptive and innate immune systems of the host. Sbi domains I and II (Sbi-I and Sbi-II) bind IgG. Sbi domain IV (residues 198–266) binds the central complement protein C3. When linked to Sbi-III, Sbi-IV induces a futile consumption of complement via alternative pathway activation, whereas isolated Sbi-IV specifically inhibits the alternative pathway without complement consumption. Here we have determined the three-dimensional structure of Sbi-IV by NMR spectroscopy, showing that Sbi-IV adopts a three-helix bundle fold similar to those of the *S. aureus* complement inhibitors Efb-C, Ehp, and SCIN. The ^{1}H-^{15}N HSQC spectrum of Sbi-III indicates that this domain, essential for futile complement consumption, is natively unfolded, at least when isolated from the rest of Sbi. Sbi-IV and Sbi-III-IV both bind C3dg with 1:1 stoichiometry and submicromolar affinity. Despite low overall sequence identity, Sbi possesses the same residues as Efb at two positions essential for Efb-C binding to C3d. Mutation to alanine of either of these residues, Arg-231 and Asn-238, abolishes both Sbi-IV binding to C3dg and Sbi-IV alternative pathway inhibition. The almost complete conservation of Sbi-III and Sbi-IV amino acid sequences across more than 30 strains isolated from human and animal hosts indicates that the unique mechanism of Sbi in complement system subversion is a feature of infections of both humans and economically important animals.

Staphylococcus aureus is a common commensal of humans but can cause illnesses ranging from superficial skin infections to serious invasive infections such as septic arthritis, osteomyelitis, and endocarditis. The broad spectrum of diseases caused by *S. aureus* reflects not only an ability to colonize different tissues through an array of surface-bound adhesins (MSCRAMMS or microbial surface components recognizing adhesive matrix molecules) (1) but also to circumvent various immune surveillance systems, among them the complement system (2–4). Complement comprises a finely regulated cascade of proteins that links the innate and adaptive immune systems (5–7). The complement system both eliminates bacterial cells directly via the membrane attack complex and recruits effector molecules that label bacterial cells and target them for destruction by immune effector cells, for example neutrophils. This process of complement fixation occurs via two specific recognition pathways: the lectin pathway, which is a component of innate immunity and the classical pathway, which requires specific interaction with antibodies bound to antigens on target cells. The lectin and classical pathways are amplified by the alternative pathway, although the alternative pathway may also initiate on a target independent of the classical and lectin pathways. All three pathways converge on the complement protein C3, which has two disulfide-linked polypeptide chains and various proteolytic derivative forms that correspond to different intermediates in the activation cascade (8).

Numerous proteins from microbial pathogens that target the complement cascade at several points have been discovered in recent years (9), including several from *S. aureus*. These include the extracellular fibrinogen-binding protein (including the N-terminal fibrinogen binding domain and C-terminal complement inhibitory domain; Efb),[4] Ehp, SCIN, and SSL7. Efb and Ehp bind to C3 and reduce its availability at the bacterial surface (10–13). SCIN interacts with the classical and alternative pathway C3 convertases C4b2a and C3bBb at a bacterial surface and thereby reduces their enzymatic activity (14). SSL7 binds complement factor C5 and inhibits complement-medi-

* This work was supported by Wellcome Trust Grant 076124 (to S. B.), Biotechnology and Biological Sciences Research Council Research Grant BBS/B/12121 (to J. M. H. v. d. E.), and Canadian Institutes of Health Research Grant MOP-7081 (to D. E. I.). The costs of publication of this article were defrayed in part by the payment of page charges. This article must therefore be hereby marked "*advertisement*" in accordance with 18 U.S.C. Section 1734 solely to indicate this fact.

⌘ *Author's Choice*—Final version full access.

[S] The on-line version of this article (available at http://www.jbc.org) contains supplemental Figs. S1–S3.

The atomic coordinates and structure factors (codes 2jvg and 2jvh) have been deposited in the Protein Data Bank, Research Collaboratory for Structural Bioinformatics, Rutgers University, New Brunswick, NJ (http://www.rcsb.org/).

[1] Supported by a BBSRC Ph.D. studentship.

[2] To whom correspondence may be addressed. Tel.: 44-0-1225-383639; Fax: 44-0-1225-386779; E-mail: bssjmhve@bath.ac.uk.

[3] To whom correspondence may be addressed. Tel.: 44-0-1225-386436; Fax: 44-0-1225-386779; E-mail: bsssb@bath.ac.uk.

[4] The abbreviations used are: Efb, extracellular fibrinogen-binding protein; Sbi, *S. aureus* binder of immunoglobulin; AP, alternative pathway; CP, classical pathway; Efb-C, complement inhibitory C-terminal domain of Efb; Ehp, Efb homologous protein; HSQC, heteronuclear single quantum coherence; IC_{50}, half-maximal inhibitory concentration; ITC, isothermal titration calorimetry; NOE, nuclear Overhauser effect; NOESY, nuclear Overhauser effect spectroscopy; r.m.s.d., root mean square deviation; RU, response units; Sbi-I, Sbi domain I (42–94); Sbi-II, Sbi domain II (92–156); Sbi-III, Sbi domain III (150–205); Sbi-III-IV, Sbi domains III and IV (150–266); Sbi-IV, Sbi domain IV (198–266); Sbi-E, Sbi domains I-IV (28–266); SCIN, staphylococcal complement inhibitor; SpA, *Staphylococcus* protein A; SPR, surface plasmon resonance; TEV, tobacco etch virus; TOCSY, total correlation spectroscopy; MES, 4-morpholineethanesulfonic acid; PDB, Protein Data Bank.

ated hemolysis and serum-killing of *Escherichia coli* (15). There are also several *S. aureus* proteins that inhibit neutrophil movement to the infection site (16–20). Among these, CHIPS (chemotaxis inhibitory protein of *S. aureus*) blocks the neutrophil receptors for the major chemoattractants C5a (a by-product of complement activation) and fMLP (17, 20).

Another *S. aureus* immune subversion protein, Sbi, was originally identified as an IgG-binding (21) and β_2-glycoprotein-I-binding (22) protein. Sbi is a 436-amino acid protein that occurs in many *S. aureus* strains, including methicillin-sensitive (MSSA) and methicillin-resistant (MRSA) strains. From its N terminus, Sbi comprises four small domains up to residue 266 followed by eight copies of a P*XXXX* repeat motif with a high concentration of glutamine, lysine, aspartate, valine, and isoleucine and then a C-terminal tyrosine-rich 130-residue region. Unlike *Staphylococcus* protein A, the other known *S. aureus* IgG-binding protein (2), Sbi lacks the typical Gram-positive cell wall-anchoring sequence LP*X*TG. Indeed, evidence using Western blots of fractionated cells from several *S. aureus* strains, including Newman, indicates that most Sbi is secreted into the medium (23).

We have recently demonstrated that Sbi is a multifunctional protein that not only interferes directly with the adaptive immune system through its two N-terminal IgG binding domains (Sbi-I and Sbi-II) (24), but also modulates the innate immune system through its third and fourth domains (Sbi-III and Sbi-IV) (23). Specifically, Sbi binds complement protein C3 through Sbi-IV interaction with C3 subunits C3dg and C3a and induces a futile consumption of complement predominantly via fluid phase activation of the alternative pathway. Sbi fragments containing domains I-II-III-IV (Sbi-E) and III-IV induce this futile consumption of complement, whereas isolated Sbi-IV does not. Sbi-IV is nevertheless strongly inhibitory in an assay measuring alternative pathway activation (23).

Here, we have determined the solution structure of Sbi-IV, showing that it resembles the structures of Efb C-terminal domain (12), Ehp (13), SCIN (25), and domains of SpA (26). Site-directed mutagenesis, binding experiments, and complement assays have been carried out to investigate the role of Sbi-IV in Sbi subversion of the complement system.

EXPERIMENTAL PROCEDURES

Cloning, Expression, and Purification of Recombinant Sbi Fragments—DNA sequences encoding several Sbi fragments were amplified by PCR using *S. aureus* strain Mu50 genomic DNA as template and cloned into a pET-based vector with a TEV-cleavable N-terminal hexahistidine tag (27), as described previously (23, 24). The resulting plasmids were used to transform *E. coli* strain BL21(DE3). Cells were grown at 37 °C to an A_{600} value of 0.6 when they were induced by addition of isopropyl-1-thio-β-D-galactopyranoside (Melford) to 0.2 mM and cultured for a further 4 h. ^{15}N-labeled Sbi-III and ^{15}N-labeled and ^{15}N/^{13}C-labeled Sbi-IV for NMR spectroscopy were produced by expression in minimal medium with $^{15}NH_4Cl$ and $^{15}NH_4Cl$/$^{13}C_6$-D-glucose (Spectra Stable Isotopes) as the sole nitrogen and nitrogen/carbon sources. Following cell harvest by centrifugation and lysis by sonication, the lysate was centrifuged at 40,000 × *g* for 15 min, and the supernatant filtered through a 0.45-μm filter. Sbi fragments were purified by nickel ion-chelating chromatography using a 1-ml HisTrap column attached to an ÁKTA purifier (GE Healthcare). The column was then washed with binding buffer, and the bound proteins were eluted using a 0.05–1.0 M imidazole gradient. For NMR data acquisition, the N-terminal hexahistidine tag was removed by incubation with TEV protease (Invitrogen), and the hexahistidine tag-free Sbi fragment was then separated from TEV protease (itself His-tagged) by a second passage through a HisTrap column. Following TEV removal of the hexahistidine tag, the Sbi proteins contained N-terminal residues GAM from the expression vector.

NMR Sample Generation and NMR Spectroscopy of Sbi-III and Sbi-IV—Purified Sbi-III and Sbi-IV were exchanged into 5 mM MES, 100 mM NaCl, 1 mM EDTA, 1 mM benzamidine, pH 5.5. All NMR data were acquired at 16 °C on a Varian Unity INOVA spectrometer operating at a nominal proton frequency of 600 MHz, using a triple resonance 5-mm probe equipped with *z*-axis-pulsed-field gradients. NMR data were processed using the NMRPipe/NMRDraw software suite (28) and analyzed using CCPN Analysis (29). Sequence-specific backbone resonance assignments of Sbi-IV were made using three-dimensional HNCACB, CBCA(CO)NH, HNCO, HN(CA)CO, HNHA, and HBHA(CBCACO)NH data sets. Side chain resonance assignments of Sbi-IV were made using CCC-TOCSY-NNH, HCC-TOCSY-NNH, HCCH TOCSY, and ^{15}N-edited TOCSY (12.1, 12.1, 15.6, and 50 ms mixing times). ^{1}H chemical shifts were referenced to DSS. ^{15}N and ^{13}C chemical shifts were referenced indirectly to DSS (30). Sbi-IV NOE distance restraints were obtained by analysis of ^{15}N-NOESY HSQC (50, 100, and 150 ms mixing times) and ^{13}C-NOESY HSQC (70 and 175 ms mixing times) spectra. All pulse sequences were from the Varian BioPack suite of pulse sequences.

Structure Calculation—NOE peak intensities were converted to distance restraints within Analysis. Distances involving methyl groups, aromatic ring protons, and non-stereospecifically assigned methylene protons were represented as a $(\Sigma r^{-6})^{-1/6}$ sum (31). Backbone dihedral angles ϕ and ψ were predicted from $^{13}C_\alpha$, $^{13}C_\beta$, $^{13}C'$, $^{1}H_\alpha$, and backbone ^{15}N chemical shifts using TALOS (32). The ϕ dihedral angles were restrained to TALOS-predicted values ±30° or ±40°, and ψ dihedral angles were restrained to TALOS-predicted values ±50°. Hydrogen bond distance restraints were established from NOE patterns, and the proximities of donor and acceptor groups in structures calculated using NOE-derived distance restraints. For hydrogen bond restraints, the NH-O distance was assigned lower and upper distance bounds of 1.5 and 2.5 Å, and the N-O distance assigned lower and upper distance bounds of 2.5 and 3.5 Å.

Structures were calculated using the Python interface of Xplor-NIH 2.18 (33, 34), using simulated annealing starting from random extended structures. Default values were used for all force constants and molecular parameters. Ensembles of NMR structures were analyzed for violated restraints using the VMD-Xplor visualization package (35). The structure determination was carried out iteratively whereby consistently violated restraints were reassigned, wherever possible, using existing structures or removed until a consistent set of constraints was

obtained with few violations in the ensemble. The ensemble of structures was further refined with Xplor-NIH standard refinement protocols using the final set of restraints. The quality of the structures was assessed using PROCHECK-NMR (36).

Site-directed Mutagenesis of Sbi-IV—Sbi-IV R231A and N238A single mutants and R231A-N238A double mutant were made using the QuikChange site-directed mutagenesis kit (Stratagene). The following oligonucleotide primers (MWG Biotech AG) were used to make the Sbi-IV R231A and N238A mutations: 5′-CAA TTG AAA ACA GAG CTT TAG CAC AAC GAG AAG-3′ (forward primer), 5′-CTT CTC GTT GTG CTA AAG CTC TGT TTT CAA TTG-3′ (reverse primer), 5′-GCA CAA CGA GAA GTT GCC AAA GCA CCT ATG GAT GTA AAA GAG-3′ (forward primer), 5′-CTC TTT TAC ATC CAT AGG TGC TTT GGC AAC TTC TCG TTG TGC-3′ (reverse primer). The mutant proteins were expressed and purified as described above for wild-type Sbi-IV.

Isothermal Titration Calorimetry—Isothermal titration calorimetry experiments were done at 25 °C using a VP-ITC calorimeter (Microcal) in a very similar way to that described for Efb-C3 measurements (12). Sbi-IV, Sbi-III-IV, and C3dg were exchanged into 20 mM Tris, 150 mM NaCl, pH 8.0. For each interaction, reciprocal experiments were done, one with C3dg in the cell and Sbi-IV or Sbi-III-IV in the syringe and the other with Sbi-IV or Sbi-III-IV in the cell and C3dg in the syringe. The concentration of protein in the cell ranged between 10.4 and 19 μM, and the concentration of protein in the syringe ranged between 156 and 203 μM. A 1-μl injection of protein into the cell was followed by multiple injections of 5 μl at 4-min intervals, and the evolved heat was measured. All data were fit using Origin software (OriginLab) as described (12).

Serum Affinity Pulldown Assay—Purified Sbi-I-II, Sbi-II, Sbi-III, Sbi-IV, Sbi-IV R231A, Sbi-IV N238A, and Sbi-IV R231A-N238A were each covalently coupled to a 1-ml NHS-activated Sepharose High Performance column (GE Healthcare) according to the manufacturer's instructions. After equilibration with phosphate-buffered saline (PBS), 5 ml of human serum (Cambrex) was applied to the column. Columns were washed with PBS, and bound proteins were eluted with a 0–1 M NaCl gradient over 10 ml. The binding of serum proteins was analyzed by SDS-PAGE. Size exclusion chromatography, with a Superdex-200 gel filtration column (GE Healthcare), was used for further purification of the bound fragments. Trypsinized protein fragments from excised gel slices were analyzed by MALDI-TOF. ProteinLynx software was used for protein identification.

Surface Plasmon Resonance—Surface plasmon resonance experiments were performed on a Biacore X (Biacore, Piscataway, NJ) instrument at 25 °C in HEPES-buffered saline (10 mM HEPES, pH 7.2, 3 mM EDTA, 150 mM NaCl, 0.005% (v/v) surfactant P-20 (Biacore)). 800 resonance units (RU) of C3dg were immobilized on a CM-5 sensor chip (Biacore) by standard amino coupling chemistry following the manufacturer's protocol, with a reference channel being sham-activated and deactivated. Wild-type or mutant Sbi-IV analytes were injected at a flow rate of 20 μl/min for 60 s at the concentrations indicated in Fig. 6, followed by a 60-s buffer flow before initiating the washing phase. The sensor chip was regenerated between successive analyte injections with a 60-s pulse of 2 M NaCl, which brought the sensorgram signal back to baseline.

TABLE 1
Structural statistics on the NMR-derived structures of Sbi-IV

Total number of NOE restraints		1116
Intraresidue		320
Sequential/med. range (i to $i + 1 - 4$)		621
Long range		175
Number of dihedral angle restraints		138
Number of hydrogen bond restraints		78
R.m.s.d. for backbone atoms[a]		0.29 Å
R.m.s.d. for non-hydrogen atoms[a]		0.93 Å
Average numbers of NOE violations		
>0.5 Å (per structure)		1.5
Average number of dihedral angle violations		
>5° (per structure)		0
	Average structure	**Ensemble**
Ramachandran plot regions[b]		
Most favored (%)	88.4	92.4
Additional allowed (%)	11.6	7.6
Generously allowed (%)	0.0	0.0
Disallowed (%)	0.0	0.0

[a] The r.m.s.d. from the mean structure calculated over residues 201–222, 228–238, and 245–261.
[b] Calculated with PROCHECK-NMR (36).

Complement Assays—The Wielisa Total Complement System Screen (Wieslab), described by Seelen *et al.* (37), was used to measure inhibition of the alternative complement pathway by a range of concentrations of Sbi-IV, Sbi-IV R231A, Sbi-IV N238A, and Sbi-IV R231-N238A, using a procedure similar to that described previously (23). Briefly, wild-type or mutant Sbi-IV was added to a particular concentration in human serum, and assayed for complement activity after 30 min of preincubation at 37 °C. The assay was completed in duplicate, according to the manufacturer's instructions, and included a blank, a positive control (human serum from healthy individuals), and a negative control (heat-inactivated serum). Inhibition of complement activation was quantified from absorbance at 405 nm using the calculation (sample − negative control)/(positive control − negative control) × 100%.

RESULTS

Sbi-IV Structure Determination—A semi-automated procedure for iterative NOE assignment was used to determine the structure of Sbi-IV. The final structures were generated using 1116 NOE-derived distance restraints (comprising 320 intraresidue, 621 sequential and medium range, and 175 long range NOEs where long range means between amino acids five or more apart in the sequence), 78 hydrogen bond restraints and 138 ϕ and ψ dihedral angle restraints (68 ϕ and 70 ψ) (Table 1). The ensemble of 20 simulated annealing structures selected from 50 calculations on the basis of lowest energy, and the average structure, are shown in Fig. 1. Over the regular secondary structure elements, the ensemble of structures has a backbone r.m.s.d. from the mean of 0.29 Å and an r.m.s.d. of 0.93 Å for all non-hydrogen atoms. A Ramachandran plot of the structures with PROCHECK-NMR (36) indicates that 100% of the residues (excluding Gly and Pro residues) lie in the most favored or additionally allowed regions (Table 1).

Sbi-IV Forms a Three-Helix Bundle—Sbi-IV adopts a three-helix bundle fold (Fig. 1) with approximate overall dimensions

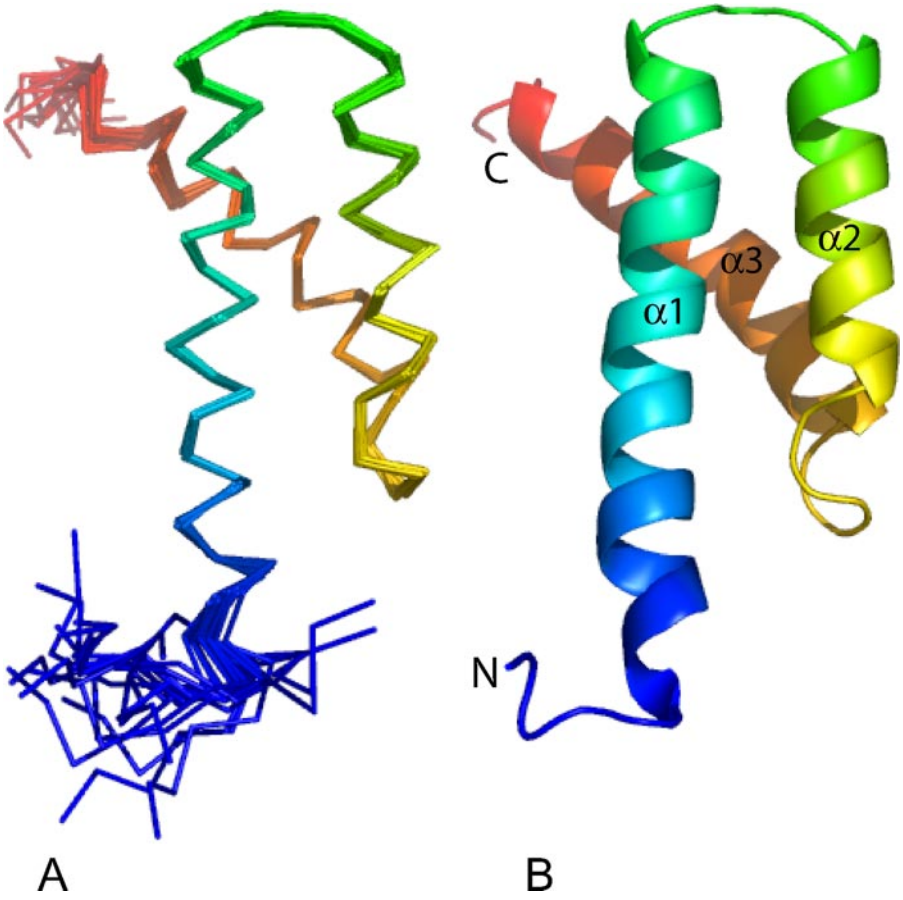

FIGURE 1. **Structure of Sbi-IV.** *A*, backbone (N, C^{α}, and C′) trace of the 20 lowest energy structures colored as a continuum from *blue* at the N terminus to *red* at the C terminus. *B*, *ribbon diagram* of the average structure colored as in *A*. The α-helices and N and C termini are labeled. This figure was generated using PyMol.

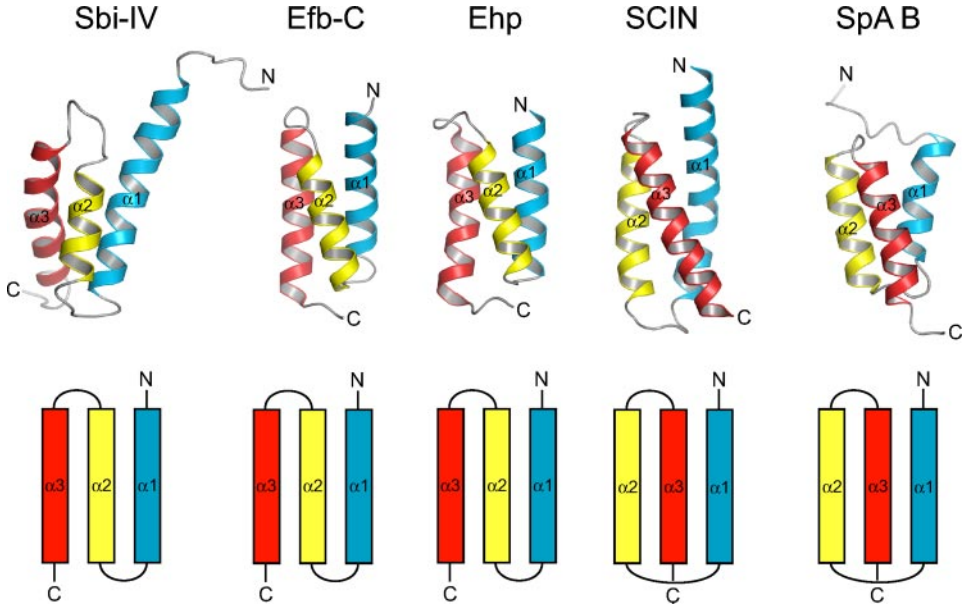

FIGURE 2. **Structural comparison of *S. aureus* immune modulator proteins.** Sbi-IV (PDB code 2jvh), Efb-C (PDB 2gom), Ehp (PDB 2noj), SCIN (PDB 2qff), and protein A domain B (PDB 1ss1) are shown in *ribbon* and *schematic topology* representations. Helix α1 is *blue*, α2 is *yellow*, and α3 is *red*. This figure was generated using PyMol.

of 45 Å × 25 Å × 25 Å. Helix α1 (residues Glu-201 to Asn-222) is connected by a loop to helix α2 (residues Glu-228 to Asn-238), which is connected by a loop to helix α3 (residues Lys-245 to Ala-261). The N-terminal six residues and C-terminal three residues are disordered. None of the residues 198–206 and 257–266 is involved in long range NOEs, and these residues make essentially no contribution to the tertiary structure of the domain. The core of the bundle comprises hydrophobic residues with hydrophilic side chains oriented toward solvent. A similar three-helix bundle fold has been observed in the other *S. aureus* complement modulatory proteins Efb-C (12), Ehp (13), SCIN (25), and SpA (26) (Fig. 2).

Isolated Sbi-III Is Unfolded—The ^{1}H-^{15}N HSQC spectrum of Sbi-III contains 52 backbone NH peaks (supplemental Fig. S1). This compares with 56 peaks expected based on the amino acid sequence of the construct including the three N-terminal residues, GAM, from the expression vector. This almost exact 1:1 correspondence with the expected number of peaks indicates that Sbi-III adopts a single conformation in solution, but the narrow ^{1}H chemical shift dispersion, with every backbone NH peak except three located in the range 8.0–8.5 ppm, indicates that this conformation lacks significant tertiary structure, *i.e.* Sbi-III is natively unfolded. The peak patterns in the ^{1}H-^{15}N HSQC spectra of Sbi-IV (supplemental Fig. S2) and Sbi-III-IV (supplemental Fig. S3) indicate that Sbi-III remains unfolded in the presence of Sbi-IV. We cannot preclude, however, the possibility that Sbi-III adopts a different conformation in full-length Sbi where its conformation may be influenced by one or more of the other domains.

Sbi-IV and Sbi-III-IV Bind C3dg with 1:1 Stoichiometry—Thermodynamics of the interactions between Sbi-IV and C3dg and between Sbi-III-IV and C3dg were measured by reciprocal (Sbi:C3dg and C3dg:Sbi) isothermal titration calorimetry experiments (Fig. 3 and Table 2). The ITC results indicate that the stoichiometry of both Sbi-IV:C3dg and Sbi-III-IV:C3dg interactions is 1:1 with K_d values of 0.35 μM and 0.28 μM (averages of results from reciprocal ITC titrations). These affinities are lower

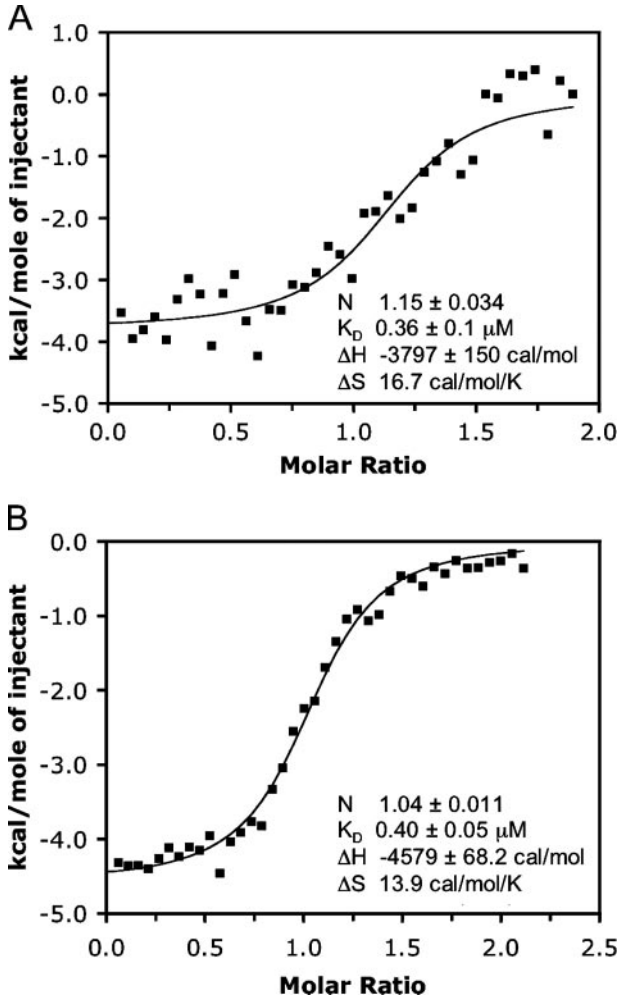

FIGURE 3. **Isothermal titration calorimetry analyses of the Sbi-IV:C3dg (*A*) and Sbi-III-IV:C3dg (*B*) interactions.** In *A*, the concentration of C3dg in the cell was 10.4 μM, and the concentration of the Sbi-IV injectant in the syringe was 203 μM. In *B*, the concentration of C3dg in the cell was 12.0 μM, and the concentration of the Sbi-III-IV injectant in the syringe was 173 μM. In each case, the data were fit to a single class of binding site model, and the best fit parameters for N (stoichiometry), K_d, and Δ*H*, along with the error estimates of the fit, are provided as an *inset* to each panel. Δ*S* is a secondarily calculated value, and thus there is no error estimate. The reciprocal experiments in which C3dg was titrated into Sbi-IV or Sbi-III-IV were also performed (results summarized in Table 2).

than the nanomolar to subnanomolar C3dg affinities previously measured by SPR and ITC for Efb-C (12) and Ehp (13).

Efb Residues Important for C3d Binding Align with the Corresponding Residues in Sbi-IV—The sequence identity between Sbi-IV (69 residues) and Efb-C (72 residues) is only 19% over a 43-residue stretch, with five of eight identical residues located in helix α2 (Fig. 4). Despite the low sequence identity, Sbi-IV helix α2 residues Arg-231 and Asn-238 align with two Efb residues, Arg-131 and Asn-138, that are particularly important for formation of the Efb-C-C3d complex (12). Two other Efb residues that contact C3d, His-130 and Lys-135, are conservatively substituted by arginines in Sbi-IV. In the Efb-C-C3d complex, Arg-131 lies deep in an acidic pocket of C3d, and Asn-138 is involved in an intermolecular hydrogen bonding network. Alignment with Arg-131 and Asn-138 of Efb suggests that Sbi residues Arg-231 and Asn-238 are key residues for Sbi interaction with C3.

R231A and N238A Mutations Abolish Sbi-IV Binding to C3dg—As a consequence of the sequence alignment results mentioned in the previous section, Sbi-IV R231A and Sbi-IV N238A single mutants and Sbi-IV R231A-N238A double mutant were made. As shown by affinity pulldown experiments, both single and double mutations effectively abolished binding between Sbi-IV and C3dg-containing C3 derivatives present in serum (Fig. 5). This was confirmed in an SPR experiment (Fig. 6), where the binding interaction between Sbi-IV and biosensor-bound C3dg was abolished when any of the Sbi-IV single or double mutants was used as an analyte. A similar effect was previously observed upon double mutation of Efb residues Arg-131 and Asn-138 (12), but the results of similar experiments with Ehp were complicated by the presence of a second lower affinity binding site on Ehp (13). At about 0.6 μM when Sbi-IV is the analyte (this study, data not shown) and 0.8 μM when C3dg is the analyte (23), the wild-type Sbi-IV:C3dg affinity measured by SPR is slightly lower than the 0.35 μM affinity measured by ITC (see above). This may simply reflect the superimposed surface effects of SPR due to the need to chemically couple one of the binding partners to the biosensor surface, relative to the pure solution phase interaction measured in the ITC experiment.

TABLE 2

Assessment of C3dg binding to Sbi-III-IV and Sbi-IV by isothermal titration calorimetry

Titrant	Cell	*n*[a]	K_d	Δ*H*	Δ*S*
			μM	*kcal/mol*	*cal/mol/K*
Sbi-III-IV	C3dg	1.04	0.40	−4.6	13.9
Sbi-IV	C3dg	1.15	0.36	−3.8	16.7
C3dg	Sbi-III-IV	0.92	0.17	−3.9	17.8
C3dg	Sbi-IV	0.93	0.34	−4.6	14.0

[a] *n*, molar ratio of titrant molecule bound to ligand molecule in the cell at satration.

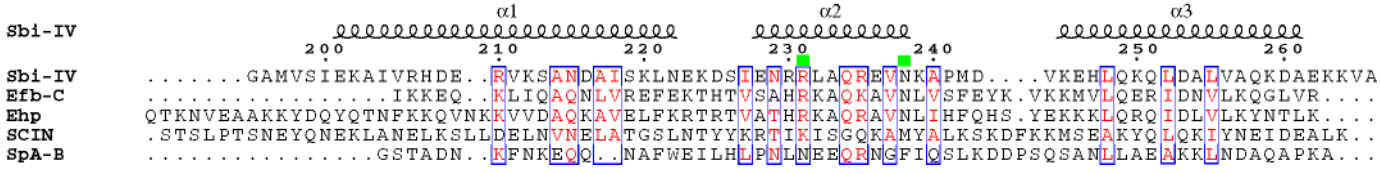

FIGURE 4. **Sequence alignment of Sbi-IV, Efb-C, Ehp, SCIN, and SpA-B.** The secondary structure elements of Sbi-IV are shown. The amino acid sequence numbers are for Sbi-IV. Sbi-IV residues Arg-231 and Asn-238 are highlighted by *green rectangles*; the corresponding Efb-C residues are Arg-131 and Asn-138, and the corresponding Ehp residues are Arg-75 and Asn-82.

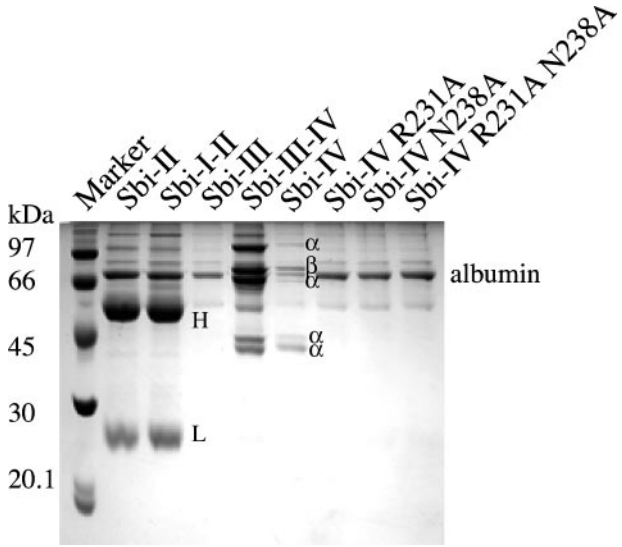

FIGURE 5. **Serum affinity pulldown assay.** SDS-PAGE analysis of an affinity pulldown assay with human serum as prey and various individual and combined Sbi domains as bait proteins immobilized on an NHS-Sepharose column. Captured proteins were identified by MALDI-TOF. The first lane is a ladder of molecular weight marker proteins with molecular weights indicated. The next two lanes show capture of IgG heavy- (*H*, ~50 kDa) and light-chain (*L*, ~25 kDa) fragments by Sbi-II and Sbi-I-II. The *fourth lane* shows that Sbi-III fails to capture IgG and C3. The *fifth* and *sixth lanes* show that Sbi-III-IV and Sbi-IV capture fragments of complement component C3 with approximate molecular masses of 119, 75, 65, 43, and 40 kDa (C3 chain origin of the fragments is indicated). The last *three lanes* show that Sbi-IV mutants R231A, N238A, and R231A-N238A fail to capture C3 and instead capture albumin.

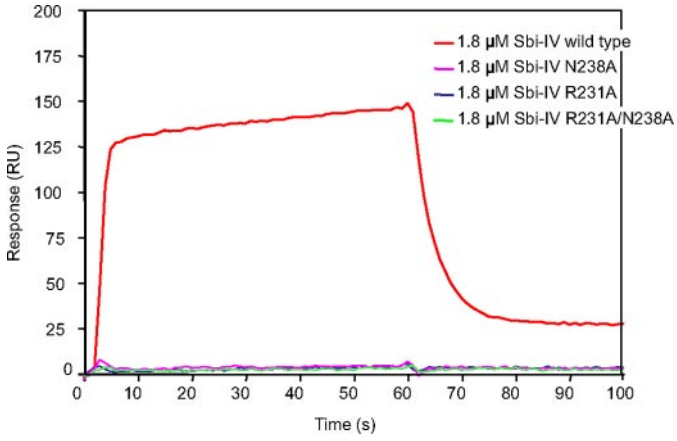

FIGURE 6. **Surface plasmon resonance analysis of Sbi-IV:C3dg binding.** SPR sensorgrams are shown for Sbi-IV wild-type and Sbi-IV mutants R231A, N238A, and R231A-N238A.

R231A and N238A Mutations Abolish Sbi-IV Inhibition of the Alternative Complement Pathway—Sbi-IV inhibited the alternative pathway in a dose-dependent manner (Fig. 7). All of the R231A, N238A, and R231A-N238A mutations abolished Sbi-IV inhibition of the alternative pathway (Fig. 7) in the same way that double mutation of Efb residues Arg-131 and Asn-138 abolished alternative pathway blockade by Efb (12). The IC_{50} value for Sbi-IV alternative pathway inhibition was ~10 μM compared with 0.56 μM for Efb, 0.41 μM for Efb-C (12) and 0.12 μM for Ehp (13).

DISCUSSION

S. aureus has evolved a complement system subversion strategy incorporating several secreted proteins that inhibit the

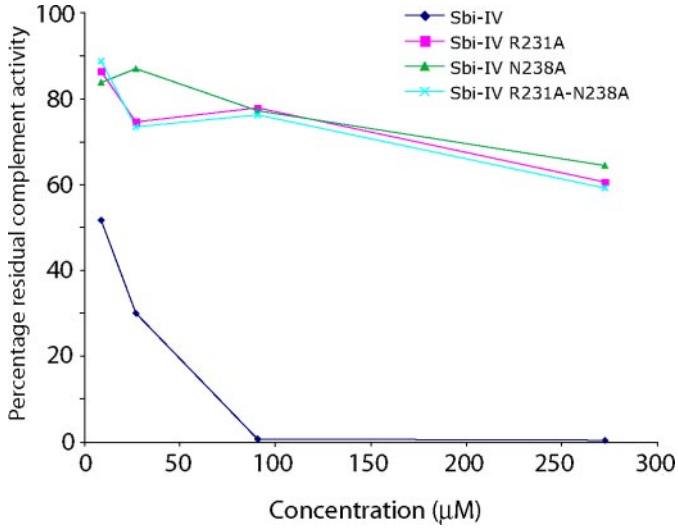

FIGURE 7. **Sbi-IV inhibition of the alternative complement pathway.** Dose response residual complement activity for Sbi-IV and Sbi-IV mutants R231A, N238A, and double mutant R231A-N238A were assessed in a Wielisa assay.

complement cascade at different points using a variety of mechanisms (9–11, 13–15, 17, 20, 38). Sbi is one such protein (23), although it was originally discovered in the late 1990s as a binder of IgG (21) and β_2-glycoprotein I (22), a membrane adhesion protein implicated in blood coagulation. The same authors subsequently showed that expression of Sbi is induced by human IgG (39). We have recently characterized in some detail the IgG binding properties of Sbi but have found no evidence that Sbi binds β_2-glycoprotein I (24).

Sbi modulates both the adaptive and innate immune systems (23, 24). Sbi can form a precipitate with human IgG through interaction between the first two Sbi domains and Fc of IgG. This contrasts with SpA-mediated formation of insoluble immune complexes, which involves Fab in addition to Fc (24). Innate immune modulation involves the third and fourth Sbi domains: Sbi-IV and Sbi-III-IV are both able to bind the central protein of the complement system, C3, through its thioester-containing C3dg and anaphylatoxin C3a subunits. Sbi-III-IV and Sbi-E (containing domains I through IV) both activate the alternative pathway, leading to rapid consumption of C3, whereas neither Sbi-III nor Sbi-IV in isolation significantly activates complement (23); Sbi-IV, indeed, inhibits the alternative pathway in a dose-dependent fashion (Fig. 7). In this respect, Sbi-IV resembles Ehp, which specifically inhibits the alternative pathway (13), and Efb, which operates predominantly on the alternative pathway (12).

Sbi-IV is structurally similar to Efb-C (12), Ehp (13), SCIN (25), and domains of SpA (Figs. 1 and 2). Mutation of either or both of Sbi-IV residues Arg-231 and Asn-238 to alanine, moreover, essentially abolishes both Sbi-IV binding to C3dg (Figs. 5 and 6) and Sbi-IV inhibition of the alternative complement pathway (Fig. 7). The correlation between abolition of C3dg binding and abolition of alternative pathway inhibition as a result of R231A and N238A mutations further establishes the importance of direct Sbi-C3 interaction for complement subversion by Sbi (23). The effect of the R231A and N238A mutations also indicates that the mode of interaction between Sbi-IV

and C3dg has similarities with that observed for Efb-C in the crystal structure of its complex with C3d (12), although the sequence identity between Sbi-IV and Efb-C of 19% makes it difficult to assess whether Sbi and Efb have evolved a similar interface with C3d by convergent or divergent evolution. Notably, both Efb and Sbi have a binding preference for native C3 over C3b (12, 23). Analysis of the Ehp-C3d interaction by mutation and isothermal titration calorimetry indicated that Ehp has two binding sites for C3d, a high affinity site resembling that of Efb and a low affinity site that retains an asparagine corresponding to Asn-238 in Sbi and Asn-138 in Efb but lacks the arginine corresponding to Sbi Arg-231/Efb Arg-131 (13). This two site binding by Ehp was ascribed to the presence of tandem repeats of -AQ(K/R)AVNL-. Although there is a repeat of sorts in Sbi-IV (-RVKSAND- at positions 210–216 and -AQREVNK- at positions 233–239), the repeat similarity is much weaker and sequence spacing between the repeats is four residues longer than in Ehp. As expected then, analysis of the Sbi-IV:C3dg and Sbi-III-IV:C3dg interaction by ITC (Fig. 3) indicates that the stoichiometry is 1:1 (with K_d values of 0.35 μM and 0.28 μM for Sbi-IV:C3dg and Sbi-III-IV:C3dg), and as was the case in our earlier SPR measurements of the binding affinity between Sbi-IV and C3dg (23), the ITC data were well fit to a single class of binding site model.

The IC_{50} value for Sbi-IV inhibition of the alternative pathway is 10 μM compared with 0.56 μM for Efb, 0.41 μM for Efb-C (12) and 0.12 μM for Ehp (13), indicating that Sbi-IV is less efficient as an inhibitor of the alternative pathway than Efb and Ehp. The previously measured IC_{50} values for Sbi-III-IV and Sbi-E were 0.1 μM and 2 μM (23), the lower values than Sbi-IV reflecting the occurrence of rapid C3 consumption in addition to inhibition of the alternative pathway. Taken together, the affinity and IC_{50} results suggest that, while the mutation data discussed above imply that the Sbi-IV-C3 and Efb-C3 interactions share important characteristics, there are also differences that may have functional significance.

The role of Sbi-III in Sbi function is intriguing. Sbi-III does not bind C3 and ^{1}H-^{15}N HSQC NMR spectra indicate that isolated Sbi-III is natively unfolded, and it remains so when combined with Sbi-IV in the Sbi-III-IV construct, yet the presence of Sbi-III is essential for Sbi activation of the alternative pathway with resulting consumption of C3. (Any effect of other domains of Sbi on the conformation of Sbi-III remains to be investigated.) When Sbi-III-IV but not Sbi-IV is incubated with serum, a significant fraction of the C3 activated becomes covalently bound to Sbi-III-IV, presumably via the C3d thioester. Thus it seems that Sbi-III provides the transacylation target hydroxyl group for Sbi-C3b covalent adduct formation (only the nascently activated C3b form of C3 can undergo covalent adduct formation). A hypothesis as to how Sbi-III:C3 covalent adduct formation leads to C3 consumption has been proposed (23). Specifically, the Sbi-III:C3 adduct may provide a nidus for the assembly of the alternative pathway C3 convertase, C3bBb, that is at least transiently resistant to inactivation by the serum regulatory molecules fH and fI, thereby facilitating the consumptive cleavage of C3. The N-terminal domains Sbi-I and Sbi-II may further assist in the complement consumption process by recruiting IgG molecules that are also suitable targets for transacylation by C3b. Previous studies have shown that alternative pathway C3 convertases covalently attached to IgG are in a protected environment with respect to their rate of inactivation by fH and fI (40, 41).

To date the C3 binding characteristics of Sbi, Efb (11, 12), and Ehp (13) have been examined using recombinant proteins generated from *S. aureus* strains isolated from human patients. We have compared the nucleotide sequences of 23 *sbi* genes from a sample of 28 strain isolates from human and animal (pig, cow, goat, ewe, rabbit, and poultry) hosts plus those from five complete genome sequences (24). No changes at all occurred in Sbi-III and very few changes occurred in Sbi-IV. The positions of the Sbi-IV polymorphic amino acids (222–224 and 244–246) correspond to the loop between helices α1 and α2 and the α2-α3 loop and N terminus of helix α3. This conservation of Sbi-III and Sbi-IV amino acid sequences across more than 30 strains isolated from human and animal hosts suggests that the unique mechanism of complement system subversion by Sbi is a feature of both human and animal infections.

Identification of the structures and active sites of the small complement inhibitory proteins secreted by *S. aureus* has lead to consideration of the potential therapeutic exploitation of these proteins (9), including Efb (12), Ehp (13), and SCIN (25). Like Efb and Ehp, it appears that a discrete region of the surface of Sbi-IV involving a handful of residues forms the interface with C3, the central protein of the complement system. Sbi-IV itself is therefore a potentially attractive basis either for structure-based design of small molecule or peptide-based therapeutic molecules or for development of protein-based therapeutics for complement-mediated acute inflammatory diseases.

Acknowledgements—We thank Prof. M. C. Enright (Imperial College London) for providing S. aureus genomic DNA. The Wellcome Trust is acknowledged for purchase of the 600 MHz NMR spectrometer (Grant 051902) used in this study.

REFERENCES

1. Foster, T. J., and Höök, M. (1998) *Trends Microbiol.* **6,** 484–488
2. Foster, T. J. (2005) *Nat. Rev. Microbiol.* **3,** 948–958
3. Rooijakkers, S. H. M., van Kessel, K. P. M., and van Strijp, J. A. G. (2005) *Trends Microbiol.* **13,** 596–601
4. Rooijakkers, S. H. M., and van Strijp, J. A. G. (2007) *Mol. Immunol.* **44,** 23–32
5. Walport, M. J. (2001) *New Engl. J. Med.* **344,** 1058–1066
6. Walport, M. J. (2001) *New Engl. J. Med.* **344,** 1140–1144
7. Carroll, M. C. (2004) *Nat. Immunol.* **5,** 981–986
8. Sahu, A., and Lambris, J. D. (2001) *Immunol. Rev.* **180,** 35–48
9. Lambris, J. D., Ricklin, D., and Geisbrecht, B. V. (2008) *Nat. Rev. Microbiol.* **6,** 132–142
10. Lee, L. Y. L., Höök, M., Haviland, D., Wetsel, R. A., Yonter, E. O., Syribeys, P., Vernachio, J., and Brown, E. L. (2004) *J. Infect. Dis.* **190,** 571–579
11. Lee, L. Y. L., Liang, X. W., Höök, M., and Brown, E. L. (2004) *J. Biol. Chem.* **279,** 50710–50716
12. Hammel, M., Sfyroera, G., Ricklin, D., Magotti, P., Lambris, J. D., and Geisbrecht, B. V. (2007) *Nat. Immunol.* **8,** 430–437
13. Hammel, M., Sfyroera, G., Pyrpassopoulos, S., Ricklin, D., Ramyar, K. X., Pop, M., Jin, Z., Lambris, J. D., and Geisbrecht, B. V. (2007) *J. Biol. Chem.* **282,** 30051–30061
14. Rooijakkers, S. H. M., Ruyken, M., Roos, A., Daha, M. R., Presanis, J. S., Sim, R. B., van Wamel, W. J. B., van Kessel, K. P. M., and van Strijp, J. A. G.

(2005) *Nat. Immunol.* **6,** 920–927
15. Langley, R., Wines, B., Willoughby, N., Basu, I., Proft, T., and Fraser, J. D. (2005) *J. Immunol.* **174,** 2926–2933
16. Chavakis, T., Hussain, M., Kanse, S. M., Peters, G., Bretzel, R. G., Flock, J. I., Herrmann, M., and Preissner, K. T. (2002) *Nat. Med.* **8,** 687–693
17. Postma, B., Poppelier, M. J., van Galen, J. C., Prossnitz, E. R., van Strijp, J. A. G., de Haas, C. J. C., and van Kessel, K. P. M. (2004) *J. Immunol.* **172,** 6994–7001
18. Prat, C., Bestebroer, J., de Haas, C. J. C., van Strijp, J. A. G., and van Kessel, K. P. M. (2006) *J. Immunol.* **177,** 8017–8026
19. Bestebroer, J., Poppelier, M., Ulfman, L. H., Lenting, P. J., Denis, C. V., van Kessel, K. P. M., van Strijp, J. A. G., and de Haas, C. J. C. (2007) *Blood* **109,** 2936–2943
20. Wright, A. J., Higginbottom, A., Philippe, D., Upadhyay, A., Bagby, S., Read, R. C., Monk, P. N., and Partridge, L. J. (2007) *Mol. Immunol.* **44,** 2507–2517
21. Zhang, L. H., Jacobsson, K., Vasi, J., Lindberg, M., and Frykberg, L. (1998) *Microbiology* **144,** 985–991
22. Zhang, L. H., Jacobsson, K., Strom, K., Lindberg, M., and Frykberg, L. (1999) *Microbiology* **145,** 177–183
23. Burman, J. D., Leung, E., Atkins, K. L., O'Sheaghdha, M. N., Lango, L., Bernardo, P., Bagby, S., Svergun, D. I., Foster, T. J., Isenman, D. E., and van den Elsen, J. M. H. (2008) *J. Biol. Chem.* **283,** 17579–17593
24. Atkins, K. L., Burman, J. D., Chamberlain, E. S., Cooper, J. E., Poutrel, B., Bagby, S., Jenkins, A. T. A., Feil, E. J., and van den Elsen, J. M. H. (2008) *Mol. Immunol.* **45,** 1600–1611
25. Rooijakkers, S. H. M., Milder, F. J., Bardoel, B. W., Ruyken, M., van Strijp, J. A. G., and Gros, P. (2007) *J. Immunol.* **179,** 2989–2998
26. Sato, S., Religa, T. L., Daggett, V., and Fersht, A. R. (2004) *Proc. Natl. Acad. Sci. U. S. A.* **101,** 6952–6956
27. Sheffield, P., Garrard, S., and Derewenda, Z. (1999) *Prot. Express. Purif.* **15,** 34–39
28. Delaglio, F., Grzesiek, S., Vuister, G. W., Zhu, G., Pfeifer, J., and Bax, A. (1995) *J. Biomol. NMR* **6,** 277–293
29. Vranken, W. F., Boucher, W., Stevens, T. J., Fogh, R. H., Pajon, A., Llinas, P., Ulrich, E. L., Markley, J. L., Ionides, J., and Laue, E. D. (2005) *Proteins-Struct. Funct. Bioinf.* **59,** 687–696
30. Wishart, D. S., Bigam, C. G., Yao, J., Abildgaard, F., Dyson, H. J., Oldfield, E., Markley, J. L., and Sykes, B. D. (1995) *J. Biomol. NMR* **6,** 135–140
31. Nilges, M. (1993) *Proteins-Struct. Funct. Genet.* **17,** 297–309
32. Cornilescu, G., Delaglio, F., and Bax, A. (1999) *J. Biomol. NMR* **13,** 289–302
33. Schwieters, C. D., Kuszewski, J. J., Tjandra, N., and Clore, G. M. (2003) *J. Magn. Reson.* **160,** 65–73
34. Schwieters, C. D., Kuszewski, J. J., and Clore, G. M. (2006) *Prog. Nucl. Magn. Reson. Spect.* **48,** 47–62
35. Schwieters, C. D., and Clore, G. M. (2001) *J. Magn. Reson.* **149,** 239–244
36. Laskowski, R. A., Rullmann, J. A. C., MacArthur, M. W., Kaptein, R., and Thornton, J. M. (1996) *J. Biomol. NMR* **8,** 477–486
37. Seelen, M. A., Roos, A., Wieslander, J., Mollnes, T. E., Sjoholm, A. G., Wurzner, R., Loos, M., Tedesco, F., Sim, R. B., Garred, P., Alexopoulos, E., Turner, M. W., and Daha, M. R. (2005) *J. Immunol. Methods* **296,** 187–198
38. Jiang, H. X., and Frank, M. M. (2004) *Mol. Immunol.* **41,** 252–253
39. Zhang, L. H., Rosander, A., Jacobsson, K., Lindberg, M., and Frykberg, L. (2000) *FEMS Immunol. Med. Microbiol.* **28,** 211–218
40. Fries, L. F., Gaither, T. A., Hammer, C. H., and Frank, M. M. (1984) *J. Exp. Med.* **160,** 1640–1655
41. Lutz, H. U., and Jelezarova, E. (2006) *Mol. Immunol.* **43,** 2–12